Imidazolate-Bridged Dicopper(II) and Copper−Zinc Complexes of a Macrobicyclic Ligand (Cryptand). A Possible Model for the Chemistry of Cu−Zn Superoxide Dismutase

Jean-Louis Pierre,*,† Pierre Chautemps,† Sidi Refaif,† Claude Beguin,† Abdelilah El Marzouki,† Guy Serratrice,† Eric Saint-Aman,‡ and Paul Rey§

Contribution from the Laboratoire de Chimie Biomimétique, LEDSS (URA CNRS 332) and Laboratoire d'Electrochimie Organique et de Photochimie Redox (URA CNRS 1210), Université Joseph Fourier, BP 53, 38041 Grenoble Cedex 9, France, and Laboratoire DRFMC/SESAM/CC, URA CNRS 1194, Centre d'Etudes Nucléaires de Grenoble, BP 85 X, 38041, Grenoble, France

Received July 20, 1994®

Abstract: The imidazolate-bridged dinuclear copper(II) (**1**) and the imidazolate-bridged heterodinuclear copper(II)−zinc(II) (**2**) complexes of a macrobicyclic ligand L (L = 1,4,12,15,18,26,31,39-octaazapentacyclo[13.13.13.$1^{6,10}$.$1^{20,24}$.$1^{33,37}$]-tetratetracontane-6,8,10,20,22,24,33,35,37-nonaene) were synthesized as possible models for superoxide dismutase (SOD). Their crystal structures determined by X-ray diffraction methods have shown that the two ions are pentacoordinated in a coordination environment that is found to be a slightly distorted trigonal bipyramid for one metal center and a distorted square pyramid for the other. The metal−N bond lengths range from 1.91 to 2.33 Å, and the distances Cu−Cu and Cu−Zn are 5.95 and 5.93 Å, respectively, slightly shorter than the value in the (Cu−Cu) SOD or in the (Cu−Zn) SOD. Magnetic measurements and ESR spectroscopy of the dicopper complex have shown an antiferromagnetic exchange interaction with a coupling constant of $-2J = 88$ cm^{-1}. From pH-dependent ESR and electronic spectroscopic studies, the two complexes have been found to be stable over very large pH ranges 4.5−12 for **1** and 6−10.5 for **2**. Electrochemical studies have indicated quasi-reversible behavior in dimethylacetamide solution for the first step of the reduction: $E_{1/2} = -0.27$ V/SCE for **1** (Cu^{II}_2/Cu^{I}_2 redox process) and $E_{1/2} = -0.31$ V/SCE for **2** (Cu^{II}/Cu^{I} redox process). The two complexes catalyze the dismutation of superoxide at biological pH, and the activity survives in the presence of bovine serum albumine. All the results indicate that complexes **1** and **2** act as good models for superoxide dismutase.

Introduction

Copper−zinc superoxide dismutase (SOD) contains in its active site an imidazolate-bridged bimetallic center with one copper(II) and one zinc(II) ion.[1] It has been found in the cytosol of eukaryotic cells, and it is believed to protect cells from the toxic effects of superoxide ions by catalyzing the dismutation reaction:[2]

$$O_2^- + [Cu^{II}] \rightarrow O_2 + [Cu^{I}] \quad (1)$$

$$O_2^- + [Cu^{I}] + 2H^+ \rightarrow H_2O_2 + [Cu^{II}] \quad (2)$$

The copper and zinc ions can be removed from the enzyme and be substituted by other metals; the dicopper derivative [Cu_2-Cu_2SOD] (dimer form) is particularly interesting since the activity of this modified enzyme is the same as that of the native enzyme.[3]

Many low molecular weight copper chelates are known to exhibit, in vitro, superoxide dismutase-like activity.[4] Unfortunately, most of them lose their activity in the presence of bovine serum albumine (BSA), which is able to mobilize the copper(II) ion from these complexes. BSA is a plasmatic protein which is one of the strongest biological chelators of cupric ions (log $K = 16.2$).

We thought that a topologically adapted macrobicyclic ligand (cryptand) would be able to induce a very strong complexation and retain the metal in the presence of BSA. On the other hand, an imidazolate-bridged bimetallic complex seemed to us more biomimetic than a mononuclear complex. Moreover, the closed structure of the ligand can induce a greater selectivity: only small additional ligands (e.g., O_2^-) have access to the copper center. Accordingly, the bicyclic structure is expected to play the role of the protein channel of SOD.[1]

Several imidazolate-bridged dicopper(II) complexes have been described, but only with open chain or monocyclic ligands.[3-14] In this field, the pioneering work of Lippard must

† Laboratoire de Chimie Biomimétique, LEDSS, Université Joseph Fourier.

‡ Laboratoire d'Electrochimie Organique et de Photochimie Redox, Université Joseph Fourier.

§ Laboratoire DRFMC/SESAM/CC, Centre d'Etudes Nucléaires de Grenoble.

® Abstract published in *Advance ACS Abstracts,* February 1, 1995.

(1) Tainer, J. A.; Getzoff, E. D.; Richardson, J. S.; Richardson, D. C. *Nature* **1983**, *306*, 284.

(2) Fridovich, I. *Annu. Rev. Biochem.* **1975**, *44*, 147.

(3) Strothkamp, K. G.; Lippard, S. J. *Acc. Chem. Res.* **1982**, *15*, 318.

(4) Gartner, A.; Weser, U. *Top. Curr. Chem.* **1986**, *132*, 1.

(5) Weser, U.; Schubotz, L. M.; Lengfelder, E. *J. Mol. Cat.* **1981**, *13*, 249.

(6) O'Young, C.-L.; Dewan, J. C.; Lillienthal, H. R.; Lippard, S. J. *J. Am. Chem. Soc.* **1978**, *100*, 7291.

(7) Coughlin, P. K.; Martin, A. E.; Dewan, J. C.; Watanabe, E.; Bulkowski, J. E.; Lehn, J.-M.; Lippard, S. J. *Inorg. Chem.* **1984**, *23*, 1004. Coughlin, P. K.; Lippard, S. J. *Ibid.* **1984**, *23*, 1446.

(8) Drew, M. G. B.; Cairns, C.; Lavery, A.; Nelson, S. M. *J. Chem. Soc., Chem. Commun.* **1980**, 1122.

(9) Drew, M. G. B.; Mac-Cann, M.; Nelson, S. M. *J. Chem. Soc., Dalton Trans.* **1981**, 1868.

(10) Drew, M. G. B.; Nelson, S. M.; Reedijk, J. *Inorg. Chim. Acta* **1982**, *64*, L189.

(11) Sato, M.; Ikeda, M.; Nakaya, J. *Inorg. Chim. Acta* **1984**, *93*, L61.

(12) Cabral, J. O.; Cabral, M. F.; Mac-Cann, M.; Nelson, S. M. *Inorg. Chim. Acta* **1984**, *86*, L15.

(13) Salata, C. A.; Youinou, M. T.; Burrows, C. J. *J. Am. Chem. Soc.* **1989**, *111*, 9278.

0002-7863/95/1517-1965$09.00/0

be emphasized; the model built with the bis(diene) ligand is undoubtedly the best approach of the $[Cu_2Cu_2SOD]$ active site described at this time.[7] Unbridged or μ-chloro-, μ-fluoro-, μ-hydroxo-, and μ-carbonato-bridged binuclear dicopper(II) complexes of macrobicyclic ligands have been described.[5-17,24]

Dicopper(I) complexes of cryptands also have been described.[18-24] This point has to be emphasized since it is important that, during the catalytic cycle of the superoxide dismutation, the metal in its reduced redox state remains firmly bound to the ligand.

Few imidazolate-bridged heterobinuclear Cu-Zn complexes have been described.[25-28] They consist of two independent mononuclear complexes, a Cu(II) and a Zn(II) complex, respectively, connected by an imidazolate bridge between the copper and zinc atoms. This implies that the break of the imidazolate bridge leads to three different molecules. Moreover, these complexes are expected to have lower stability than complexes with dinucleating macrocycles or macrobicycles.

Another important feature in the design of SOD mimics is the possibility of conformational twisting of the ligand in order to accommodate the two different redox states of the copper ions during the catalytic cycle. An adequate Cu(II)/Cu(I) redox potential must also be required between $E^\circ = -160$ mV vs NHE (-405 mV vs SCE) for O_2/O_2^- and $E^\circ = 890$ mV vs NHE (645 mV vs SCE) for O_2^-/H_2O_2.

In this paper, we report the synthesis, the X-ray crystal structure determination, the results of magnetic susceptibility, ESR, and electronic spectroscopic investigations, and the electrochemistry of two complexes of macrobicyclic ligand L (L = 1,4,12,15,18,26,31,39-octaazapentacyclo[13.13.13.$1^{6,10}$.$1^{20,24}$.$1^{33,37}$]-tetratetracontane-6,8,10,20,22,24,33,35,37-nonaene) (Figure 1): an imidazolate-bridged dicopper(II) tricationic complex $[(Cu(im)Cu)L]^{3+}$ (**1**) and an imidazolate-bridged copper-zinc tricationic complex $[(Cu(im)Zn)L]^{3+}$ (**2**). Complex **2** is the first imidazolate-bridged copper-zinc complex of a unique macrobicyclic ligand. A brief description of **2** has been preliminarily reported.[29] The relevance to SOD chemistry was examined.

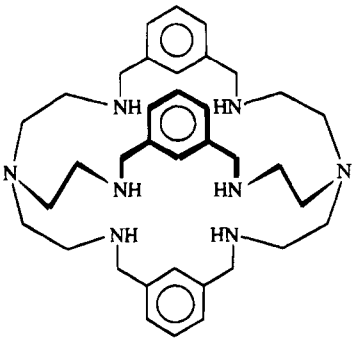

Figure 1. Structural formula of the macrobicyclic ligand L.

Table 1. Crystallographic Data for $[(Cu(im)Cu)L](ClO_4)_3$ (**1**) and $[(Cu(im)Zn)L](ClO_4)_3$ (**2**)

	1	**2**·H_2O
formula	$C_{39}H_{57}N_{10}O_{12}Cl_3Cu_2$	$C_{39}H_{59}N_{10}O_{13}Cl_3CuZn$
fw	1091.4	1111.2
space group	monoclinic $P2_1/a$	monoclinic $P2_1/a$
a (Å)	18.115(8)	18.179(8)
b (Å)	20.13(1)	20.333(9)
c (Å)	14.484(7)	15.853(6)
β (deg)	112.74(1)	113.07
V (Å^3)	5207.4	5991.17
Z	4	4
T (°C)	21	22
ϱ(calcd) (g/cm^3)	1.39	1.36
λ (Å)	0.7107	0.7107
linear abs (mm^{-1})	1.0	1.0
$R(F_o)^a$	0.098	0.103
$R_w(F_o)^b$	0.095	0.099

$^a R = \sum(F_o - F_c)/\sum wF_o$. $^b R_w = (w(F_o - F_c)^2/wF_o^2)^{1/2}$, $w = 1/(\sigma(F)^2)$.

Experimental Section

Materials and Methods. Commercial reagents were used as obtained without further purification. Solvents were purified by standard methods before use. Elemental analyses were performed by the CNRS Microanalysis Laboratory of Lyon, France.

X-ray Data Collection. The synthesis of complexes **1** and **2** afforded well-shaped crystals suitable for X-ray diffraction study. Preliminary Weissenberg photographs showed the monoclinic system. A crystal of approximate dimensions 0.2 × 0.2 × 0.2 mm^3 was mounted on an Enraf-Nonius CAD-4 four-circle diffractometer equipped with graphite-monochromated Mo Kα radiation. Accurate cell parameters were derived from least-squares fitting of the setting angles of 25 independent reflections. They are reported in Table 1 with other pertinent details regarding the structure determination. Space group $P2_1/a$ was ascertained from systematic absences, and data collection was performed at room temperature. These data were corrected for Lorentz and polarization factors but not for absorption.

Crystal Structure Determination. Structure determination was straightforward using the heavy-atom method included in the SHELX 76 package for structure determination. The positions of the non-hydrogen atoms were obtained from difference Fourier maps. These were refined with anisotropic thermal parameters. In the last refinement model, hydrogen atoms were included at calculated and fixed positions with isotropic thermal parameters equal to those of the connected carbon atoms. For **2**, both metal centers were refined as Cu^{II} ions.

Selected bond lengths and angles are reported in Tables 2 and 3. A complete listing of bond lengths (Tables SIII and SIV), bond angles (Tables SV and SVI), and anisotropic thermal parameters (Tables SVII and SVIII) are included as Supplementary Material.

Magnetic Measurements. Magnetic data were collected in the 5-300 K temperature range using a Quantum Design MPMS superconducting susceptometer working at a 0.5 T field strength. The SQUID outputs were corrected for the magnetization of the sample holder, and the molar susceptibilities were corrected for the diamagnetism of the constituent atoms by using Pascal constants.

Spectrometry. ESR spectra were recorded at 100 K on a Bruker ER 100 D spectrometer operating at 9.4 GHz with DPPH as an external

(14) Salata, C. A.; Youinou, M. T.; Burrows, C. J. *Inorg. Chem.* **1991**, *30*, 3454.
(15) Motekaitis, R. J.; Martell, A. E.; Murase, I.; Lehn, J.-M.; Hosseini, M. W. *Inorg. Chem.* **1988**, *27*, 3630 and references cited herein.
(16) Ragunathan, K. G.; Bharadwaj, P. K. *J. Chem. Soc., Dalton Trans.* **1992**, 1653.
(17) Menif, R.; Reibenspies, J.; Martell, A. E. *Inorg. Chem.* **1991**, *30*, 3446.
(18) Ngwenya, P.; Martell, A. E.; Reibenspies, J. *J. Chem. Soc., Chem. Commun.* **1990**, 1207.
(19) Jarwinski, J.; Lehn, J.-M.; Lilienbaum, D.; Zeissel, R.; Guilhem, J.; Pascard, C. *J. Chem. Soc., Chem. Commun.* **1987**, 1691.
(20) Vogtle, F.; Luer, I.; Balzani, V.; Armroli, N. *Angew. Chem., Int. Ed. Engl.* **1991**, *30*, 1333.
(21) De Mendoza, J.; Mesa, E.; Rodriguez-Ubis, J. C.; Vasquez, P.; Vogtle, F.; Windscheif, P. M.; Rissanen, K.; Lehn, J. M.; Lilienbaum, D.; Ziessel, R. *Angew. Chem., Int. Ed. Engl.* **1991**, *30*, 1331.
(22) Alberts, A. H.; Annunziata, R.; Lehn, J.-M. *J. Am. Chem. Soc.* **1977**, *99*, 8502.
(23) Youinou, M. T.; Suffert, J.; Ziessel, R. *Angew. Chem., Int. Ed. Engl.* **1992**, *31*, 775.
(24) Drew, M. G. B.; Marrs, D.; Huntert, J.; Nelson, J. *J. Chem. Soc., Dalton Trans.* **1992**, 11.
(25) Sato, M.; Nagae, S.; Uehara, M.; Nakaya, J. *J. Chem. Soc., Chem. Commun.* **1984**, 1661.
(26) Lu, Q.; Luo, Q. H.; Dai, A. B.; Hu, G. Z. *J. Chem. Soc., Chem. Commun.* **1990**, 1429.
(27) Mao, Z. W.; Yu, K. B.; Chen, D.; Han, S. Y.; Sui, Y. X.; Tang, W. X. *Inorg. Chem.* **1993**, *32*, 3104.
(28) Mao, Z. W.; Chen, D.; Tang, W. X.; Yu, K. B.; Liu, L. *Polyhedron* **1992**, *11*, 191.
(29) Pierre, J. L.; Chautemps, P.; Refaif, S. M.; Beguin, C. G.; El Marzouki, A.; Serratrice, G.; Rey, P.; Laugier, J. *J. Chem. Soc., Chem. Commun.* **1994**, 1117.

Table 2. Selected Bond Lengths (Å) and Bond Angles (deg) for $[(Cu(im)Cu)L](ClO_4)_3$ (**1**)

Cu(1)−N(1)	1.92(3)	Cu(2)−N(2)	1.91(2)
Cu(1)−N(3)	2.14(2)	Cu(2)−N(7)	2.09(2)
Cu(1)−N(4)	2.08(2)	Cu(2)−N(8)	2.12(2)
Cu(1)−N(5)	2.03(3)	Cu(2)−N(9)	2.01(2)
Cu(1)−N(6)	2.33(2)	Cu(2)−N(10)	2.27(2)
N(1)−C(1)	1.32(3)	N(2)−C(1)	1.35(5)
N(1)−C(2)	1.36(4)	N(2)−C(3)	1.38(3)
C(2)−C(3)	1.41(5)		
N(1)−Cu(1)−N(3)	91.8(9)	N(2)−Cu(2)−N(7)	94.3(9)
N(1)−Cu(1)−N(4)	94.3(9)	N(2)−Cu(2)−N(8)	89.8(9)
N(1)−Cu(1)−N(5)	169.6(1.1)	N(2)−Cu(2)−N(9)	171.2(1.0)
N(1)−Cu(1)−N(6)	109.6(1.0)	N(2)−Cu(2)−N(10)	104.6(9)
N(3)−Cu(1)−N(4)	144.1(8)	N(7)−Cu(2)−N(8)	128.8(1.0)
N(3)−Cu(1)−N(5)	82.4(1.0)	N(7)−Cu(2)−N(9)	84.9(1.0)
N(3)−Cu(1)−N(6)	102.7(9)	N(7)−Cu(2)−N(10)	114.0(8)
N(4)−Cu(1)−N(5)	85.5(1.0)	N(8)−Cu(2)−N(9)	84.0(9)
N(4)−Cu(1)−N(6)	108.4(8)	N(8)−Cu(2)−N(10)	114.1(8)
N(5)−Cu(1)−N(6)	80.2(1.0)	N(9)−Cu(2)−N(10)	83.6(9)
Cu(1)−N(1)−C(1)	130.0(2.4)	Cu(2)−N(2)−C(1)	134.3(1.7)
Cu(1)−N(1)−C(2)	125.6(1.8)	Cu(2)−N(2)−Cu(3)	122.0(2.2)
C(1)−N(1)−C(2)	104.4(2.7)	C(1)−N(2)−C(3)	103.6(2.2)
N(1)−C(2)−C(3)	109.2(2.3)	N(2)−C(3)−C(2)	107.1(2.9)
N(1)−C(1)−N(2)	115.5(2.5)		

Table 3. Selected Bond Lengths (Å) and Bond Angles (deg) for $[(Cu(im)Zn)L](ClO_4)_3$ (**2**)

Zn−N(1)	1.97(1)	Cu−N(2)	1.95(1)
Zn−N(3)	2.12(1)	Cu−N(7)	2.14(1)
Zn−N(4)	2.16(1)	Cu−N(8)	2.14(1)
Zn−N(5)	2.13(1)	Cu−N(9)	2.09(1)
Zn−N(6)	2.21(1)	Cu−N(10)	2.30(10)
N(1)−C(1)	1.33(2)	N(2)−C(1)	1.30(1)
N(1)−C(2)	1.34(1)	N(2)−C(3)	1.36(2)
C(2)−C(3)	1.36(2)		
N(1)−Zn−N(3)	94.3(5)	N(2)−Cu−N(7)	90.3(5)
N(1)−Zn−N(4)	86.7(5)	N(2)−Cu−N(8)	93.7(5)
N(1)−Zn−N(5)	166.1(5)	N(2)−Cu−N(9)	164.6(5)
N(1)−Zn−N(6)	108.3(5)	N(2)−Cu−N(10)	112.3(5)
N(3)−Zn−N(4)	123.4(5)	N(7)−Cu−N(8)	143.7(5)
N(3)−Zn−N(5)	84.3(5)	N(7)−Cu−N(10)	83.1(5)
N(3)−Zn−N(6)	116.7(5)	N(7)−Cu−N(9)	102.3(5)
N(4)−Zn−N(5)	82.5(5)	N(8)−Cu−N(9)	83.7(5)
N(4)−Zn−N(6)	116.4(5)	N(8)−Cu−N(10)	109.3(5)
N(5)−Zn−N(6)	84.5(5)	N(9)−Cu−N(10)	82.8(5)
Zn−N(1)−C(1)	130.8(9)	Cu−N(2)−C(1)	127.3(1.2)
Zn−N(1)−C(2)	125.4(1.2)	Cu−N(2)−C(2)	128.9(9)
C(1)−N(1)−C(2)	103.7(1.2)	C(1)−N(2)−C(3)	103.8(1.4)
N(1)−C(2)−C(3)	108.9(1.5)	N(2)−C(3)−C(2)	108.5(1.2)
N(1)−C(1)−N(2)	115.1(1.4)		

calibrant. The pH of the aqueous solutions was measured before the addition of dimethylsulfoxide (DMSO). DMSO was added to provide good quality glass. UV−visible spectra were obtained on a Perkin-Elmer Lambda 2 spectrophotometer with quartz cells. ^1H NMR spectra were recorded on an AC 200 Bruker spectrometer (working at 200.13 MHz) using a 5 mm probe at 25 °C. Chemical shifts were measured in parts per million from internal TMS. The proton resonance was assigned by using homonuclear decoupling. Fast-atom bombardment (FAB) mass spectra in the positive mode were recorded on a Nermag R 1010C apparatus equipped with an M scan (Wallis) atom gun (8 kV, 20 mA). The complex peak intensities were normalized to the nitrobenzyl alcohol matrix peak at $m/z = 153.9$, which is set at 100%.

Electrochemistry. The electrochemical behavior of $[(Cu(im)Cu)L]^{3+}$ and $[(Cu(im)Zn)L]^{3+}$ was examined in aqueous and in *N,N'*-dimethylacetamide (DMA) solvents. Potassium nitrate in aqueous media and tetrabutylammonium perchlorate (TBAP) in DMA were used as supporting electrolytes at a 0.1 mol·dm^{-3} concentration. The pH was adjusted at 7 for the experiments carried out in aqueous media. The electrochemical curves were recorded using a submillimolar solution prepared from the isolated complexes. The experiments were run under an inert atmosphere at room temperature. The electrochemical results were obtained through cyclic voltammetry at the hanging mercury electrode, polarography at the dropping mercury electrode, and controlled potential coulometry on a mercury pool using a PAR model 264 A polarographic analyzer equipped with a PAR model 303 A mercury drop electrode. The electrochemical curves were recorded on a Kipp-Zonen $x-y$ recorder. A conventional three-electrode cell was used in all experiments. A saturated calomel electrode (SCE), separated from the test solution by the electrolytic solution sandwiched between two fritted disks, was used as the reference electrode. All potentials are referred to it.

Superoxide Dismutase Activities. Superoxide anions were supplied to the evaluating system from the hypoxanthine−xanthine oxidase reaction as described in the literature.[30] The SOD activities were evaluated by the classical nitro blue tetrazolium (NBT) assay.[31] The concentration of complex required to yield 50% inhibition of the reduction of NBT (named IC_{50}) was determined both with and without bovine serum albumine.

Syntheses. L was prepared by the procedure described by Martell.[17] The complexes were prepared as described below.

$[(Cu(im)Cu)L](ClO_4)_3$. A solution of imidazole (680 mg, 10 mmol) in degassed methanol (40 cm^3) was added dropwise (30 min) under argon to a methanol solution (100 mL) of $Cu(ClO_4)_2{\cdot}6H_2O$ (3.7 mg, 10 mmol). The resulting blue solution was stirred for 1 h. A 14 cm^3 volume of the preceding solution (0.5 mmol of $[Cu(im)Cu](ClO_4)_3$) was added dropwise to L (300 mg, 0.5 mmol, in 30 cm^3 of methanol). Afterward, the solution was stirred for 3 h. A blue precipitate was obtained and isolated (yield: 70%). The blue powder was dissolved in acetonitrile and recrystallized by slow diffusion of ethyl acetate. Anal. Calcd for $C_{39}H_{57}N_{10}Cu_2(ClO_4)_3$: C, 42.97; H, 5.23; N, 12.85; Cu, 11.66. Found: C, 43.10; H, 5.17; N, 12.60; Cu, 11.30. FAB$^+$ MS (NBA): m/z 991 $[(M - ClO_4)^+]$, 922 $[(M - im - ClO_4)^+]$, 891 $[(M - 2ClO_4)^+]$, 823 $[(M - im - 2ClO_4)^+]$, 724 $[(M - im - 3ClO_4)^+]$, 659 $[(M - im - Cu - 3ClO_4)^+]$.

$[(Cu(im)Zn)L](ClO_4)_3$. To a solution of 208 mg (0.347 mmol) of L in acetonitrile (50 cm^3) was added 129 mg (0.347 mmol) of $Zn(ClO_4)_2{\cdot}6H_2O$ in acetonitrile (10 cm^3). After 30 min a solution of 128 mg (0.347 mmol) of $Cu(ClO_4)_2{\cdot}6H_2O$ in acetonitrile (10 cm^3) was added. The solution turned blue. After 30 min a solution of 48 mg (0.347 mmol) of imidazole in acetonitrile (10 cm^3) was added. The solution turned dark blue, was stirred for 3 h, and, becoming concentrated, led to an oil. A blue powder, precipitated upon methanol addition, was isolated and recrystallized from an acetonitrile solution by slow diffusion in ethyl acetate (yield: 70%). Anal. Calcd for $C_{39}H_{57}N_{10}CuZn(ClO_4)_3{\cdot}3H_2O$: C, 40.77; H, 5.48; N, 12.19; Cu, 5.53; Zn, 5.69. Found: C, 40.77; H, 5.41; N, 12.48; Cu, 5.40; Zn, 5.05. FAB$^+$ MS (NBA): m/z 992 $[(M - ClO_4)^+]$, 893 $[(M - 2ClO_4)^+]$, 793 $[(M - 3ClO_4)^+]$, 659 $[(M - Zn - im - 3ClO_4)^+]$. It should be pointed out that when an excess of zincic salt was used, e.g., 2 equiv, the dizinc complex $[Zn_2L](ClO_4)_4$ (white powder) was obtained, which led to the imidazolate-bridged dizinc complex $[(Zn(im)Zn)L](ClO_4)_3$ (white solid) upon addition of imidazole. The zinc complexes were further characterized by FAB$^+$ mass spectrometry and by ^1H NMR.

Results

Preparation and Characterization of $[(Cu(im)Cu)L](ClO_4)_3$ (1) and $[(Cu(im)Zn)L](ClO_4)_3$ (2). We have reproduced the procedure described by Martell[17] leading to the free macrobicyclic ligand L. Complex **1** was prepared by addition of a stoichiometric amount of L to a solution of $[Cu(im)Cu](ClO_4)_3$ in methanol:

$$L + [Cu(im)Cu](ClO_4)_3 \rightarrow [(Cu(im)Cu)L](ClO_4)_3 \quad (3)$$

The use of the preformed [Cu(im)Cu] entity had been previously described.[13,14] $[(Cu(im)Cu)L](ClO_4)_3$ was also prepared by a sequential route without isolation of the unbridged dicopper

(30) Fridovich, I. In *CRC Handbook of Methods for Oxygen Radical Research*; Greenwald, R. A., Ed.; CRC: Boca Raton, FL, 1985; p 51.

(31) Auclair, C.; Voisin, E. In *CRC Handbook of Methods for Oxygen Radical Research*; Greenwald, R. A., Ed.; CRC: Boca Raton, FL, 1985; p 123.

complex, but with a lower yield than in the process depicted by reaction 3 (imH: neutral imidazole):

$$L + 2Cu(ClO_4)_2 \rightarrow [Cu_2L](ClO_4)_4 \quad (4)$$

$$[Cu_2L](ClO_4)_4 + imH \rightarrow [(Cu(im)Cu)L](ClO_4)_3 \quad (5)$$

Complex **2** was synthesized according to the following reactions:

$$L + Zn(ClO_4)_2 \rightarrow [ZnL](ClO_4)_2 \quad (6)$$

$$[ZnL](ClO_4)_2 + Cu(ClO_4)_2 \rightarrow [(CuZn)L](ClO_4)_4 \text{ (not isolated)} \quad (7)$$

$$[(CuZn)L](ClO_4)_4 + imH \rightarrow [(Cu(im)Zn)L](ClO_4)_3 \quad (8)$$

The white monozinc complex was characterized by FAB^+ mass spectrometry and ^1H NMR. Complex **1** is blue, and complex **2** is dark blue. The target complexes were obtained in 70% yields from reactions **3** and **8**, respectively. They were first characterized by elemental analysis and FAB^+ mass spectrometry. They were precipitated in methanol and recrystallized by slow diffusion of ethyl acetate in acetonitrile solution, leading to suitable crystals for X-ray analysis. The solid complexes were again characterized by FAB^+ mass spectrometry. The use of ligand L, which does not employ imine groups (as is the case for most of the imidazolate-bridged dicopper complexes in the literature), is a warranty against degradation of the complexes in aqueous medium, especially if acidic conditions occur.

Crystal Structure Determinations. An ORTEP projection of compounds $[(Cu(im)Cu)L](ClO_4)_3$ (**1**) and $[(Cu(im)Zn)L](ClO_4)_3$ (**2**) also showing the atomic numbering is depicted in Figure 2a. The two compounds crystallize in the monoclinic space group $P2_1/a$. for $[(Cu(im)Zn)L](ClO_4)_3$, as both metal centers were refined as Cu(II) ions, the X-ray results are consistent with an average (Cu + Zn)/2 on each metal site, i.e., an average Cu(or Zn)−N(im) distance of 1.96 Å. Each atom, Cu(1) and Cu(2) or Cu and Zn, is pentacoordinated (four nitrogen atoms from L and one from imidazolate) in an arrangement intermediate between a trigonal bipyramid and a square pyramid, depending on the metal center. Analysis of the Cu and Zn coordination polyhedra according to the method of Muetterties[32] and Galy[33] provides the degree of distortion Δ from an ideal trigonal bipyramid TBP (Δ = 0) to square pyramid SP (Δ = 1). The values are calculated to be 0.55 and 0.23 for Cu(1) and Cu(2) in **1** and 0.63 and 0.20 for Cu and Zn in **2**, indicating that the geometry around one metal center is distorted toward SP having N(6) or N(10) (**1** or **2**, respectively) as the apical ligand, while the geometry around the other one is a slightly distorted TBP with atoms N(3), N(4), and N(6) or atoms N(7), N(8), and N(10) (**1** or **2**, respectively) forming the trigonal planes. For **1**, the calculations reveal that Cu(2) is located at 0.218 Å out of the mean trigonal plane toward imidazolate, whereas in **2** the value is found to be 0.235 Å for Zn. The plane of the bridged imidazolate is almost parallel to two phenyl planes (6°) (C(17)−C(22) and C(25)−C(30)) and almost perpendicular to the third phenyl plane (87°) (C(33)−C(39)).

Magnetic Properties. Magnetic data for complex **1** are reported in Figure 3 in the forms χ and χT versus T. The behavior of the magnetic susceptibility of **1** versus temperature is indicative of an antiferromagnetically coupled compound. The

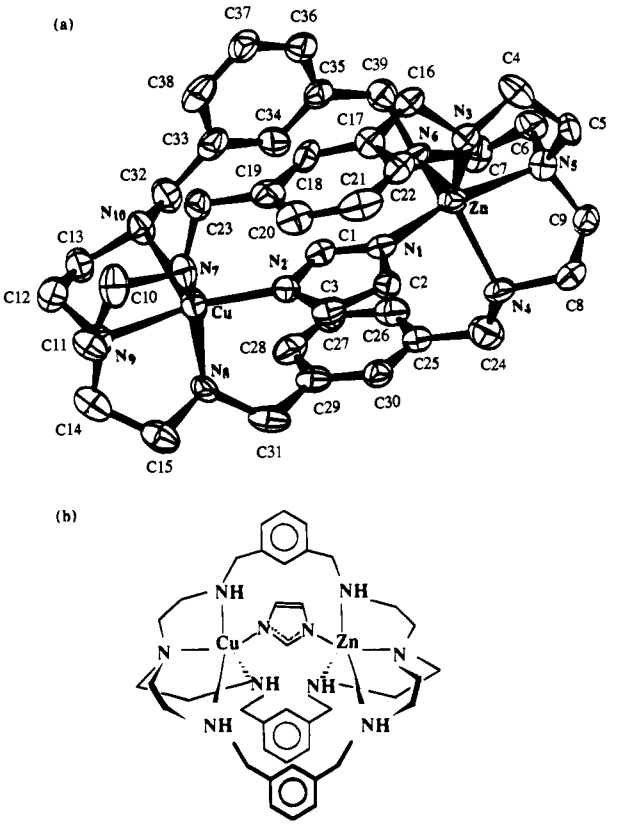

Figure 2. (a) ORTEP representation of **2** $(ClO_4)_3$ with thermal ellipsoids drawn at the 30% probability level. For **1**, Cu and Zn are replaced by Cu(2) and Cu(1), respectively. (b) Schematic representation of **2**.

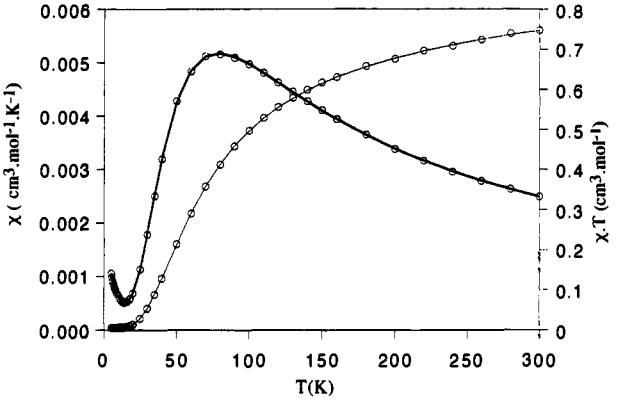

Figure 3. Temperature dependence of the magnetic susceptibility for **1** in the form χ vs T (—) and χT vs T (—). The solid lines result from a least-squares fit according to eq 9.

high-temperature χT value 0.747 $cm^3 \cdot mol^{-1}$ is very close to that expected for a two-independent-spin system ($S = {}^1/_2$). The susceptibility data were fitted to the Bleaney−Bowers equation for exchange-coupled pairs of Cu(II) ions[34] with $-2J$ the magnetic exchange parameter in the spin Hamiltonian ($H = -2JS_1 \cdot S_2$; $-2J$ is the singlet−triplet separation) and g as variable parameters:

$$\chi = 2Ng^2\beta^2/3kT[1 + {}^1/_3 \exp(-2J/KT)]^{-1} \quad (9)$$

The experimental data closely fit the Bleaney−Bowers expression as represented in Figure 3 and give the value of the magnetic exchange parameter $-2J = 88$ cm^{-1} and a g value of 2.12. As expected, the magnetic properties of complex **2** differ

(32) Muetterties, E. L.; Guggenberger, L. J. *J. Am. Chem. Soc.* **1974**, *96*, 1748.

(33) Galy, J.; Bonnet, I.; Anderson, S. *Acta Chem. Scand.* **1979**, *A33*, 383.

(34) Bleaney, B.; Bowers, K. D. *Proc. R. Soc. London, A* **1952**, *214*, 451.

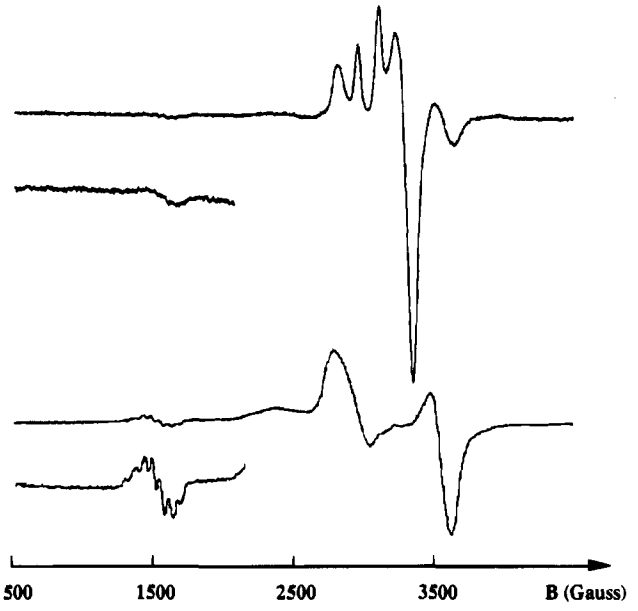

Figure 4. The ESR spectra of **1** (bottom) and **2** (top) (0.002 mol·dm^{-3}) in frozen water/dimethyl sulfoxide (DMSO) solutions (1:1, v/v) at 100 K.

markedly from those of complex **1**. The room temperature xT value is 0.374 cm^3·mol^{-1}, in agreement with a one-spin system ($S = {}^1/_2$). The xT value is roughly constant over the 120–300 K temperature range, but gradually decreases to 0.23 cm^3·mol^{-1} at 30 K. Under this temperature a constant value for χT is observed. This behavior is ascribed to a paramagnetic species containing two antiferromagnetically coupled Cu(II) ions and attributed to complex **1**. The data were fitted by taking into account magnetic susceptibility of the two species [(Cu(im)-Zn)L]$^{3+}$ and [(Cu(im)Cu)L]$^{3+}$. Their molar fractions are respectively x and $(1.05 - x)/2$ and that for the diamagnetic species [(Zn(im)Zn)L]$^{3+}$ is $(0.95 - x)/2$ on the basis of the chemical analysis that suggested an overall composition of 1.05 mol in Cu and 0.95 mol in Zn. The value of x was evaluated as 0.70, indicating that the sample contained 0.175 (molar fraction) of [(Cu(im)Cu)L]$^{3+}$ and 0.125 (molar fraction) of [(Zn-(im)Zn)L]$^{3+}$.

ESR Studies. The ESR spectra of frozen water/DMSO (1:1 v/v) solutions of complexes **1** and **2** recorded at 100 K are shown in Figure 4. Confirming the magnetic measurements, the spectra of **1** exhibit the expected spectral features of an antiferromagnetically dinuclear species; (i) The $\Delta M_s = 2$ "half-field" transition is observed with seven clearly resolved copper hyperfine lines giving a splitting of 57.2 G, and (ii) the $\Delta M_s = 1$ region shows two broad signals at 2900 and 3600 G and a very flattened signal at 2500 G characteristic of zero-field splitting effects on $g_\parallel$ and $g_\perp$ signals. The parallel and perpendicular components of the separations $d_\parallel$ and $d_\perp$, respectively, derive from

$$d_\parallel = \frac{2|D|}{g_\parallel \beta} \quad \text{and} \quad d_\perp = \frac{|D|}{g_\perp \beta} \tag{10}$$

where D is the zero-field splitting parameter. The two broad signals at 2900 and 3600 G were thus assigned to the split $g_\perp$ signal, allowing calculation of $|D|$. For $g_\parallel$ only one component at 2500 G is observed; the other is presumably overlapped by the $g_\perp$ component at 3600 G. Nevertheless, $g_\parallel$ could be determined from D. Analysis of the spectrum gave the following values: $|D| = 0.070$ cm^{-1}, $g_\parallel = 2.21$, and $g_\perp = 2.07$.

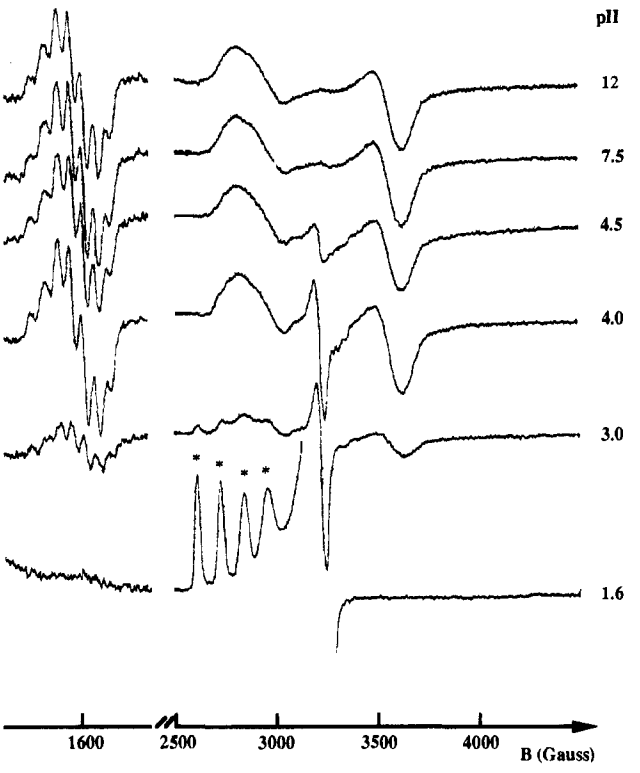

Figure 5. The ESR spectra of **1** (0.002 mol·dm^{-3}) in frozen water/DMSO solutions (1:1, v/v) at 100 K as a function of pH; peaks marked with an asterisk are Cu(II)-free.

The value of D is consistent with other dinuclear copper(II) complexes.[35]

The spectrum of complex **2** exhibits the usual line shape for mononuclear Cu(II) complexes with $g_\parallel > g_\perp > 2.03$, indicating an axial symmetry. The measured values are $g_\parallel = 2.205$, $g_\perp = 2.058$, $A_\parallel = 145 \times 10^{-4}$ cm^{-1}, and $g_\parallel/A_\parallel = 152$ cm, indicating a rather square pyramidal geometry with a $d_{x^2-y^2}$ ground state. The spectrum is very similar to that of [Cu_2Zn_2SOD] having a $g_\parallel/A_\parallel$ value of 162 cm[5,36] for which an arrangement around the copper ion intermediate between a trigonal bipyramid and a square pyramid has been postulated. In addition the spectrum exhibits another set of small signals at 1500, 2500, and 3600 G assigned to the [(Cu(im)Cu)L]$^{3+}$ species as already determined from the magnetic measurements.

Solution Stability of the Complexes 1 and 2. The pH-dependent stability of an aqueous solution of the solid complexes was studied by ESR and UV–visible spectrometry.

Complex [(Cu(im)Cu)L]$^{3+}$. The ESR spectra of **1** were recorded as a function of pH in frozen water/DMSO (1:1 v/v) solutions (Figure 5). The exceptional stability of the complex is shown by the unchanged spectrum in the pH range 4.5–12 (spectra D–F). At pH 4, spectrum C shows that **1** is the major species with a small amount of another species present which is assumed to be [Cu_2L]$^{4+}$. Indeed, the signal at 3200 G is similar to that obtained for a solution containing 1 equiv of L and 2 equiv of cupric ion at the same pH. At pH 3, free copper-(II) begins to appear in solution, as judged by ESR signals, and at pH 1.6, the spectrum exhibits only the signals of free Cu(II) ions in solution. Similar results have been obtained from UV–visible spectrometry in either water or water/DMSO solutions. In water, the spectrum displays a broad band (d–d transition)

(35) Hendriks, H. M.; Biker, P. J. M. W. L.; Verschoor, G. C.; Reedijk, J. *J. Chem. Soc., Dalton Trans.* **1982**, 623 and references cited herein. Oberhauser, K. J.; Richardson, J. F.; Buchanan, R. M.; McCusker, J. K.; Hendrickson, D. N.; Latour, J.-M. *Inorg. Chem.* **1991**, *30*, 1357.
(36) Weser, U. *Struct. Bonding (Berlin)* **1973**, *17*, 1.

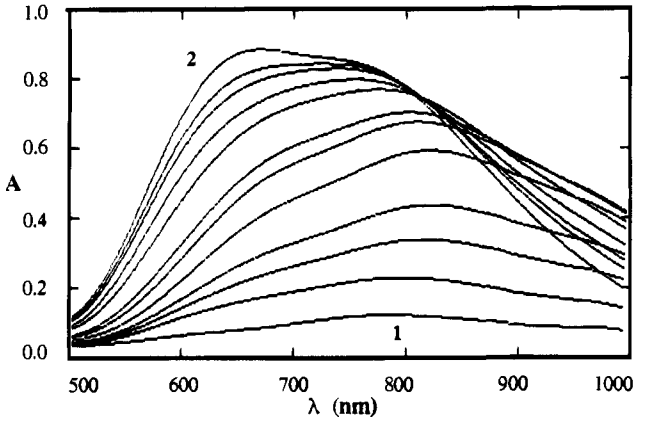

Figure 6. The electronic spectra of **1** (0.002 mol·dm^{-3}) in aqueous solution (0.1 mol·dm^{-3} KNO_3) recorded as a function of pH, from 1 to 2: pH = 2.55, 4.08, 4.34, 4.51, 4.87, 5.23, 5.39, 5.89, 6.30, 7.00, 7.48, and 8.75.

at λ_{max} = 660 nm (ϵ = 450 mol^{-1}·dm^3·cm^{-1}) with a shoulder at about 750 nm which remains unchanged in the pH range 4−12. At pH = 1.6 we observed at λ = 780 nm the broad band of Cu(II) ion in aqueous solution providing that the complex **1** is completely dissociated.

The study of the formation of complex **1** was undertaken by UV−vis spectrometry starting from the previous aqueous solution obtained at pH 1.6. The visible spectra recorded in the pH range 1.6−12 are shown in Figure 6. From pH 1.6 to about 5.0, the evolution of the spectrum was similar to that of a solution containing only Cu(II) and L in a 2:1 molar ratio. This was interpreted by the successive formation of dicopper complex $[Cu_2L]^{4+}$ and monohydroxy species $[Cu_2LOH]^{3+}$ in agreement with Menif et al.[17] The absorbance data in the pH range 4−5 were analyzed by means of a Schwarzenbach plot[37] according to the equilibrium

$$[Cu_2L]^{4+} + H_2O \overset{K_{OH}}{\rightleftharpoons} [Cu_2LOH]^{3+} + H^+ \qquad (11)$$

The value of K_{OH} was calculated to be $10^{4.46}$ in good agreement with the $10^{4.58}$ value determined from potentiometric measurements.[17] It should be noted that a hydroxide bridge between the two copper ions was assumed to be involved in the $[Cu_2LOH]^{3+}$ species.[17] Above pH 5 the visible spectrum was markedly changed. The d−d band was found to shift from λ = 820 nm to λ = 660 nm, giving at pH 8 the same spectrum as that of the isolated $[(Cu(im)Cu)L]^{3+}$ complex dissolved in aqueous solution. This evolution is thus attributed to the formation of the imidazole bridge. Then , in the pH range 8−12 the spectrum was unchanged. The complex can hence be regenerated from an acidic solution on raising the pH to about 8. The large shift of the d−d absorption band to higher energy can be explained as a consequence of a change in the coordination of Cu(II) from trigonal bipyramidal geometry (λ = 820 nm) to tetragonal (near to square pyramidal) geometry (λ = 660 nm).[38]

Complex $[(Cu(im)Zn)L]^{3+}$. ESR spectra recorded as a function of pH (Figure 7) clearly showed that the complex is stable over the pH range 6−10.5. As pH was decreased from 6 to 4.5, another set of signals appeared that are characteristic of free copper(II) ions. The spectrum at pH 2.5 indicated that the complex was completely dissociated since the corresponding signals vanished. It must be noted that at pH > 11 only the signals of complex **1** were observed. The formation of **1** could be ascribed to an exchange between one Zn(II) and one Cu(II) of two $[(Cu(im)Zn)L]^{3+}$ complexes providing the $[(Cu(im)Cu)L]^{3+}$ and the ESR-silent $[(Zn(im)Zn)L]^{3+}$ species. The UV−visible spectrum of **2** in aqueous solution is quite similar to **1**, exhibiting a broad band at λ_{max} = 640 nm (ϵ = 200 mol^{-1}·dm^3·cm^{-1}) with a shoulder at 730 nm. The UV−visible spectra were not systematically investigated as a function of pH since absorption arising from complex **1** partly masked that from **2**.

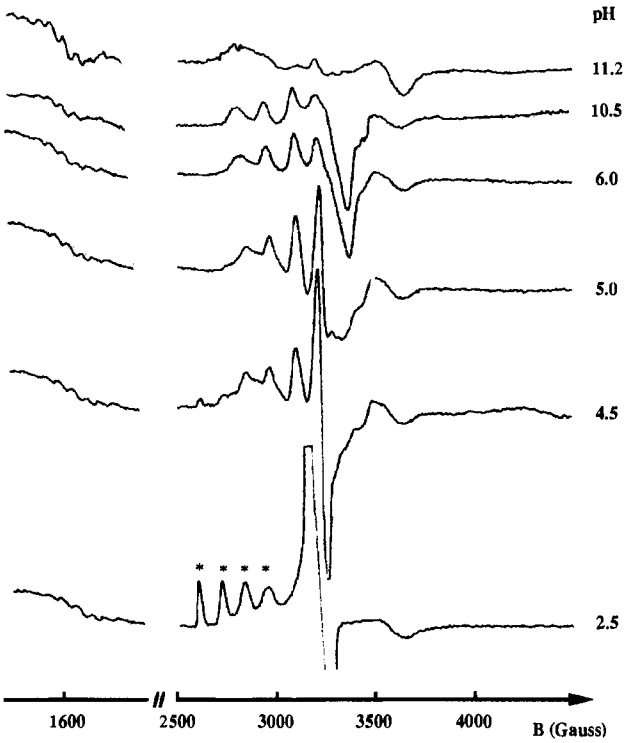

Figure 7. The ESR spectra of **2** (0.002 mol·dm^{-3}) in frozen water/DMSO (1:1, v/v) solutions at 100 K as a function of pH; peaks marked with an asterisk are Cu(II)-free.

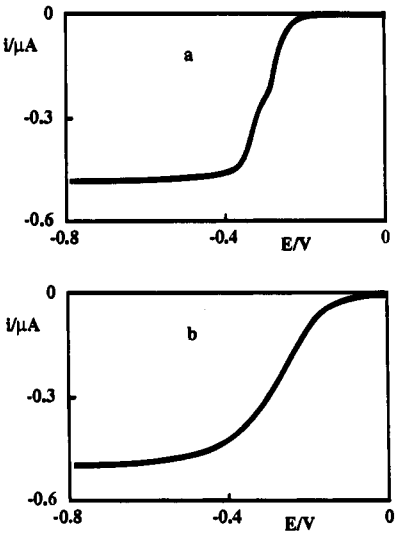

Figure 8. Dropping mercury electrode polarogram at a scan rate of 5 mV/s of **1**, 0.1 mmol·dm^{-3} in (a) aqueous solution with 0.1 mol·dm^{-3} KNO_3 at pH = 7 and (b) DMA solution with 0.1 mol·dm^{-3} TBAP, V vs SCE.

Electrochemistry. The polarographic behavior of $[(Cu(im)Cu)L]^{3+}$ in aqueous media is characterized by two cathodic waves having close half-wave potentials at −0.27 and −0.34 V/SCE, respectively (Figure 8a). The separation between these

(37) Schwarzenbach, G.; Schwarzenbach, K. *Helv. Chim. Acta* **1963**, *46*, 1390.

(38) Hathaway, B. J. *J. Chem. Soc., Dalton Trans.* **1972**, 1196.

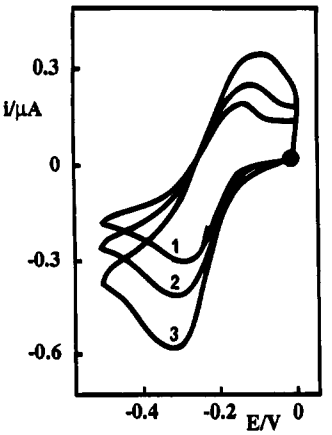

Figure 9. Cyclic voltammetry at the HME of **1** in DMA solution (1 mmol·dm^{-3}) with 0.1 mol·dm^{-3} TBAP; v = 50 mV/s (1), 100 mV/s (2), and 200 mV/s (3), V vs SCE.

two waves is not good enough to obtain the mixed-valence complex $[(Cu^{II}(im)Cu^{I})L]^{2+}$ by controlled potential electrolysis. In addition, an exhaustive electrolysis run at −0.7 V/SCE led to n = 3 exchanged electrons although the height of the two waves shows that the overall process corresponds to a bielectronic one. Thus, the reduced complex undergoes a slow decomposition in free Cu(I) and $[Cu^{I}(im)]L$. Disproportionation of the free Cu(I) in aqueous media leads to Cu(0) and free Cu(II) which is reduced in Cu(0) at −0.7 V/SCE. In addition, the cyclic voltammetry curve exhibits an ill-behaved peak system due to adsorption phenomena of the reduced species on the mercury electrode. This has precluded a thorough study of the reversibility of this process. The overall mechanism can be summarized by the following scheme:

$$[(Cu^{II}(im)Cu^{II})L]^{3+} \xrightarrow[-0.27\ V]{e^-} [(Cu^{II}(im)Cu^{I})L]^{2+} \quad (12)$$

$$[(Cu^{II}(im)Cu^{I})L]^{2+} \xrightarrow[-0.34\ V]{e^-} [(Cu^{I}(im)Cu^{I})L]^{+} \quad (13)$$

$$[(Cu^{I}(im)Cu^{I})L]^{+} \xrightarrow{slow} [Cu^{I}(im)L] + Cu^{+}_{aq} \quad (14)$$

$$2Cu^{+}_{aq} \rightarrow Cu + Cu^{2+}_{aq} \quad (15)$$

$$Cu^{2+}_{aq} \xrightarrow{2e^-} Cu \quad (16)$$

In dimethylacetamide (DMA), the electrochemical behavior of $[(Cu(im)Cu)L]^{3+}$ appears simpler. The polarogram is characterized by a unique bielectronic wave at −0.27 V/SCE corresponding to the reduction of $[(Cu^{II}(im)Cu^{II})L]^{3+}$ in $[(Cu^{I}(im)Cu^{I})L]^{+}$ (Figure 8b). The cyclic voltammetry study (Figure 9) shows that this process is quasi-reversible. The measured values of $\Delta E_p = E_{pc} - E_{pa}$ at scan rates of 50, 100, and 200 mV/s are respectively 0.17, 0.20, and 0.25 V. The same study has been performed with $[(Cu(im)Zn)L]^{3+}$. In aqueous media as in DMA, the polarogram is characterized by a monoelectronic wave ($E_{1/2}$ = −0.29 and −0.31 V/SCE, respectively) corresponding to the reduction of $[(Cu^{II}(im)Zn^{II})L]^{3+}$ in $[(Cu^{I}(im)Zn^{II})L]^{2+}$. Further reduction of this complex is observed only in aqueous media (−1.27 V/SCE). The cyclic voltammetry study shows that the first reduction is a quasi-reversible process only in DMA (ΔE_p = 0.20, 0.22, and 0.25 at scan rates of 50, 100, and 200 mV/s, respectively).

SOD Assays. $[(Cu(im)Cu)L](ClO_4)_3$ and $[(Cu(im)Zn)L](ClO_4)_3$ exhibit catalytic activity toward the dismutation of superoxide anions. Superoxide was supplied enzymatically from hypoxanthine–xanthine oxidase reaction to the evaluating system,[30] and the SOD activity was evaluated by the NBT assay.[31] The mode of generation of superoxide anions must be emphasized: it has been shown through the use of pulse radiolysis techniques for supplying superoxide anions that most of the copper compounds catalyze the dismutation with similar efficiency to that of the native SOD.[39] This is due to the fact that pulse radiolysis techniques provide O_2^- in high concentration (about 10^{-5} M), displacing the first step of the dismutation reaction to the right (reaction 1). When superoxide is provided from a biological source, the concentration is about 10^{-11} M, and only a few copper complexes exhibit SOD activity because of the reversibility of the first step of the dismutation reaction. Thus, it seemed very important to use a method providing a stationary state in superoxide of low concentration. The SOD activities exhibited by the two complexes survive in a bovine serum albumine solution. This result clearly shows that L is a stronger chelator of copper(II) and zinc(II) ions than BSA. The IC_{50} values of 0.5 μmol·dm^{-3} determined for the two complexes are higher than the value exhibited by native SOD (0.04 μmol·dm^{-3}), but of the same order of magnitude as the values of the best SOD mimics described in the literature.

Discussion

The structures of the two complexes $[(Cu(im)Cu)L]^{3+}$ and $[(Cu(im)Zn)L]^{3+}$ are quite similar. As expected, the metal–nitrogen bond lengths are very close for both metal sites in each complex. The M–N(im) bonds (M = Cu for **1**, M = Cu or Zn for **2**) are the shortest of all the M–N bonds, i.e., 1.91 and 1.92 Å in **1** and 1.95 and 1.97 Å in **2**, in agreement with the values in other Cu(im)Cu complexes described in the literature.[3,14] Interestingly, the bonds Cu–N(6) and Cu–N(10) (2.33 and 2.27 Å in **1** and 2.30 Å in **2**) arising from the bridge of the ligand having one phenyl plane (C(33)–C(38)) perpendicular to the other two are significantly longer than the other Cu–N bonds. This can reflect weaker bonding between the ion and the nitrogen atom. The N–C and C–C bonds in the imidazolate anion range from 1.30 to 1.41 Å and the bond angles from 103.6° to 115.5°, which are fairly close to the corresponding values in other imidazolate-bridged complexes. The same applies for the M–N–C(1) angles, which range from 127.3° to 130.8° except for the Cu(1)–N(1)–C(1) angle in L, the value of which, 134.3°, is larger than those generally observed. From comparison with literature data, it can be concluded that the Cu(im)Cu moiety has structural parameters which show small variability as a function of the geometry of the chelating ligand (two mononucleating ligands or one dinucleating ligand). Furthermore, the distances between the two metal centers have been calculated to be 5.95 and 5.93 Å in **1** and **2**, respectively. These values are slightly shorter than the value in SOD, in which the Cu(II) and Zn(II) ions lie 6.3 Å apart. A cavity size of approximately 6 Å must be allowed by the conformational changes of the macrobicyclic ligand. This implies a backbone flexible enough to accommodate the imidazolate-bridged group quite efficiently, as does the ligand L. As proof of the great importance of the steric strain of the ligand, we have tried unsuccessfully to prepare an imidazolate-bridged dicopper(II) complex of a macrobicyclic ligand L′ containing iminoethyl groups in place of the aminoethyl in L.[40] This result was to be ascribed to geometrical factors rather than to the soft binding character of the imine nitrogens. Indeed, a dicopper(II) complex

(39) Czapski, G.; Goldstein, S. *Free Radical Res. Commun.* **1988**, *4*, 225.

(40) El Marzouki, A. Ph.D. Thesis, Université Joseph Fourier, Grenoble, France, 1993.

of L′ was easily prepared. It was characterized by UV−visible and ESR spectrometry. The spectral parameters were found to be consistent with two independent Cu(II) ions having a trigonal bipyramidal environment. It should be noted that similar spectroscopic parameters were found for Cu_2L and Cu_2L'. Interestingly, the imidazolate ring lies between two phenyl rings (C(17)−C(22) and (C(25)−C(30)) and is parallel to their planes, showing a stacking effect, whereas the other phenyl plane (C(33)−C(38)) is perpendicular. Finally, the picture that emerges from the structure of the two complexes is one of a pocket formed by the macrobicycle including the Cu(im)Cu or the Cu(im)Zn moiety. It is expected that this geometry ensures a high stability for the Cu(im)Cu moiety and allows good selectivity toward substrates in relation to the SOD activity.

From the ESR spectral parameters a coordination geometry around Cu(II) near to square pyramidal with a $d_{x^2-y^2}$ ground state is strongly suggested for both complexes **1** and **2** ($g_{\|}$ = 2.21, $g_{\perp}$ = 2.07 and $g_{\|}$ = 2.205, $g_{\perp}$ = 2.058, $A_{\|}$ = 145.10^{-4} cm^{-1}, respectively) following the criteria proposed by Bencini et al.[41] to discriminate between square pyramidal and trigonal bipyramidal geometry in five-coordinated complexes. This is slightly different than in the solid state, presumably as a result of a less-constrained geometry in the frozen solution than in the solid state leading to the same coordination geometry for the two ions in solution. The electronic spectra are in agreement with the geometry deduced from ESR parameters. They exhibit absorption maxima at 660 or 640 nm (**1** or **2**) for d−d transitions as expected in square pyramidal geometry.[38] It should be pointed out that the $[Cu_2Zn_2SOD]$ exhibits quite similar spectral parameters for Cu(II).

The value of the magnetic exchange parameter $-2J$ reflects the degree of interaction between the two unpaired electrons through the bridging imidazolate ligand and is related to the overlap of the magnetic orbitals,[42] depending thus on the structural parameters of the complex. For imidazole-bridged dicopper complexes, $-2J$ values have been reported to vary from 0 to 163 cm^{-1}.[3] The magnitude of J has been shown to depend particularly on the angle α between the two Cu−N(im) bonds and on the dihedral angle θ between the imidazolate ring and the copper coordination plane.[43] The value of $-2J$ in **1**, 88 cm^{-1}, is larger than the values in numerous bridged-imidazolate complexes with either two chelating units[6,28] or a macrocyclic ligand[7,13] and in the modified bovine erythrocyte SOD $[Cu_4BESOD]$ (52 cm^{-1}).[44] This can be explained by taking into account the crystallographic data even if slight structural change has to occur in frozen solution. The α values of 162° and 166° are relatively large in comparison with other similar complexes. The θ dihedral angles were evaluated as approximately 75° by considering a square pyramidal geometry with N(1), N(4), N(5), and N(6) as the basal plane for Cu(1). These values of α and θ in **1** are thus found to favor the overlap of the $d_{x^2-y^2}$ magnetic orbital and imidazolate N orbitals leading to an enhanced antiferromagnetic interaction.

The reduction potentials of **1** and **2** from Cu(II) to Cu(I) in aqueous and DMA solutions are significantly lower than the more recent values 0.115 and 0.075 V/SCE obtained at pH 7.4 for the bovine enzyme and for the human enzyme, respectively,[45] but in the good range for O_2^- dismutation. Our values, −0.27 V for **1** and −0.29 V for **2**, are found to be in the same range as those determined in the literature for imidazolate-bridged dicopper complexes of macrocyclic ligands: −0.435 V,[13] −0.395 V,[12] and −0.235 V.[12] In complex **1** the two Cu(II) are structurally independent since they are reduced at an identical (in DMA) or nearly identical (in water) potential. The main result of the electrochemical study is the quasi-reversible behavior in aqueous solution and in DMA of the complexes **1** as a $[(Cu^{II}(im)Cu^{II})L]^{3+}/[(Cu^{I}(im)Cu^{I})L]^{+}$ redox process whereas complex **2** exhibits a $[(Cu^{II}(im)Zn^{II})L]^{3+}/[(Cu^{I}(im)Zn^{II})L]^{2+}$ redox process that has been found to be reversible in DMA. In contrast, the bis(diene)-derived imidazolate-bridged dicopper complex exhibited an irreversible reduction process (in acetonitrile) ascribed to the instability of the cuprous derivative,[6] and the only imidazolate-bridged copper zinc derivative that was studied revealed an irreversible reduction process in DMSO.[25] The reversible behavior for **1** and **2** implies that the cryptand framework is able to accommodate the geometrical change from Cu(II) to Cu(I). This process is presumed to involve either a four-coordinated or a five-coordinated Cu(I). Indeed, the Cu^{II}/Cu^{I} redox process involving five coordinations for the two copper states has been already shown on mononuclear complexes.[46] In our case, the reduction to Cu(I) complex is assumed to result in a lengthening of the Cu−N bonds to better fit the copper ion. It is, however, difficult to deduce the coordination number of Cu(I). An element of the answer can be obtained from the crystal structure of the two complexes. It clearly shows that the bridged arm with a phenyl ring perpendicular to the other two leads to surprisingly long Cu−N bond lengths (about 2.30 Å), revealing weaker bonds. One can suppose that these bonds are broken during the reduction of the complex giving rise to four-coordinated copper. This assumption can be related to the SOD activity of the two complexes. The mechanism of dismutation of superoxide anion by native SOD has been found to involve binding of O_2^- to copper in place of a bound water molecule as the fifth coordinated group. Since hexacoordination in a superoxo complex seems difficult to envisage owing to the geometry of the macrobicyclic ligand, the binding of O_2^- to **1** or **2** could thus be explained as a consequence of one labile copper−nitrogen coordination mimicking the labile copper−water coordination in native SOD.

Conclusion

The two complexes that have been synthesized appear to be good models for the active site in $[Cu_2Cu_2SOD]$ and $[Cu_2Zn_2$-SOD]. $[(Cu(im)Cu)L]^{3+}$ and $[(Cu(im)Zn)L]^{3+}$ exhibit similar several features in common with $[Cu_2Cu_2SOD]$ and $[Cu_2Zn_2$-SOD] subunits, respectively, and are good models for the physical properties of the protein active sites. In particular the ESR and electronic spectral parameters are close to those of the proteins. Electrochemical studies have evidenced a quasi-reversible process in the first step of reduction, as is the case for the proteins. The reduction potentials of our models are significantly lower than for the proteins; nevertheless the dismutation of superoxide remains thermodynamically allowed. One of the main results of this study is the large pH range stability of the imidazolate bridge and, thus, for the complexes in solution, from 4.5 to 12 for $[(Cu(im)Cu)L]^{3+}$ and from 6 to 10.5 for $[(Cu(im)Zn)L]^{3+}$. It is similar to the pH range stability for the proteins and significantly better than for the abiotic models described in the literature (pH from 6 to 10 for the best model previously described for [CuCuSOD][6] and pH from 10 to 12 for the imidazolate-bridged copper−zinc models[28]).

(41) Bencini, A.; Bertini, I.; Gatteschi, D.; Scozzafava, A. *Inorg. Chem.* **1978**, *17*, 3196.
(42) Kahn, O. *Angew. Chem., Int. Ed. Engl.* **1985**, 834.
(43) Benelli, C.; Bunting, R. K.; Gatteschi, D.; Zanchini, C. *Inorg. Chem.* **1984**, *23*, 3074.
(44) Fee, J. A.; Briggs, R. G. *Biochim. Biophys. Acta* **1975**, *400*, 439.
(45) Azab, H. A.; Banci, L.; Borsari, M.; Luchinat, C.; Sola, M.; Viezzoli, M. S. *Inorg. Chem.* **1992**, *31*, 4649.
(46) Goodwin, J. A.; Stanbury, D. M.; Wilson, L. J.; Eigenbrot, C. W.; Scheidt, W. R. *J. Am. Chem. Soc.* **1987**, *109*, 2979.

The two complexes catalyze the dismutation of superoxide at biological pH. The activity survives bovine serum albumine in contrast to almost all the SOD mimics in the literature.

The macrobicyclic structure of L with its eight nitrogen atoms provides a very stable environment for the $[Cu(im)Cu]^{3+}$ and $[Cu(im)Zn]^{3+}$ moieties. Furthermore, the ligand is able to accommodate the two Cu(I) and Cu(II) redox states without large conformational change owing to the flexibility of the tris-(2-aminoethyl)amine moiety. Complexes **1** and **2** provide interesting models to study the mechanism of O_2^- dismutation. Further investigations are now in progress.

Acknowledgment. This work was supported by a research grant awarded by EEC (Grant EUREKA SODA 437). We are grateful to Laboratories Esteve (Barcelone, Spain) and Chauvin S.A. (Montpellier, France) for their financial support and interest in this work. Dr. P. Seta (LMPM, UMR 9987 CNRS, Montpellier, France) is gratefully acknowledged for SOD assays.

Supplementary Material Available: Tables SI−SX of crystallographic data and experimental parameters, bond lengths, bond angles, anisotropic thermal parameters, and positional parameters and B_{eq} values for **1** and **2** (18 pages); Tables SXI and SXII of structure factors for **1** and **2** (20 pages). This material is contained in many libraries on microfiche, immediately follows this article in the microfilm version of the journal, can be ordered from the ACS, and can be downloaded from the Internet; see any current masthead page for ordering information and Internet access instructions.

JA942369S